All-electron *ab initio* self-consistent-field study of electron transfer in scanning tunneling microscopy at large and small tip-sample separations: Supermolecule approach

Abbas Farazdel* and Michel Dupuis
Scientific and Engineering Computations, IBM Corporation, Department 48B/MS 428, Kingston, New York 12401
(Received 11 January 1991)

Electron transfer expressed in the context of molecular-orbital theory is used as a model for scanning tunneling microscopy. We calculate the electronic coupling matrix element T_{ab}, ubiquitous in theories of electron transfer, by means of *ab initio* self-consistent-field wave functions for a supermolecule made up of a "sample" molecule and a "tip" metal atom. We find that T_{ab} varies with the lateral position of the tip, with the tip-sample distance, and with the applied bias voltage. The features of the T_{ab} curves are analyzed in terms of molecular orbitals.

I. INTRODUCTION

Scanning tunneling microscopy (STM), introduced by Binnig and Rohrer[1] in 1982, has emerged as an extraordinary method to yield a direct three-dimensional real-space image of surfaces with atomic resolution. The surface may be metallic, semiconducting, or covered with adsorbed and chemisorbed atoms and molecules.[2]

A probe metal tip is placed a few angstroms from the conducting sample surface and, with a bias voltage of $V \simeq 1$ V applied between the tip and the sample, the tunneling current $I \simeq 1$ nA across the vacuum gap is measured. In the so-called constant-current mode, V is fixed at some operating voltage and the tip-sample distance is adjusted so that the current I remains constant. In this case, as the tip scans laterally along the sampled surface, its path describes a topograph of the sample. There are, of course, other modes of operation in STM and each one "images" different properties of the sample. For example, the nature of the local electronic state of the sample can be obtained from voltage dependence of I or dI/dV at a specified tip position. The latter method is often referred to as scanning tunneling spectroscopy (STS).

Despite the tremendous experimental successes of STM-STS, the imaging mechanism itself stands in need of a consistent and tractable theoretical model which can provide a qualitative and quantitative understanding. Initial theoretical efforts go back to Baratoff[3] and Tersoff and Hamann[4,5] with reasonable success in describing some characteristics of STM-STS images. Although these and some later authors[6,7] invoke different properties of the tip or the sample in their models, their theories are primarily based on Bardeen's celebrated transfer-Hamiltonian model[8] for tunneling. The latter uses perturbation theory, which implies a large tip-sample separation equivalent to a high and large tunneling potential barrier. In addition, Bardeen assumes that the tail of the tip wave function overlaps with that of the sample to only a small extent. The model is not obviously suitable at either small tip-sample distances ($< \simeq 3$ Å) or for cases in which the tip and/or sample wave functions do not have just tails in the area between the tip and the sample. At small tip-sample distances the contribution of nontunneling electronic states to the current may be significant. Recently, however, several STM-STS theoretical models have been developed which do not depend on Bardeen's theory. In some of these models the tip is treated separately from the sample with inclusion of some tip-sample interaction potential,[9–13] while in other models the tip and the sample are treated as a whole.[14] In the spirit of the latter, we present here a theoretical model which we term the supermolecule approach to STM-STS. It is suitable for both large and small tip-sample separations; tip and sample are treated as a whole and are allowed to adjust to the presence of one another. This model is based on an *ab initio* description of electron transfer in which the initial and the final state of the supermolecule (the tip and sample aggregate) are represented by self-consistent-field (SCF) all-electron wave functions. We calculate the electron coupling matrix element T_{ab}, which enters in any theoretical treatment of electron transfer. Specifically, we seek to establish the relationship between surfaces of constant T_{ab} and the electronic structure of the "sample." In Sec. II we describe the general features of our model along with computational details. Results and related discussions are presented in Sec. III.

II. THE THEORETICAL MODEL: SUPERMOLECULE APPROACH

The underlying physics STM-STS is basically electron tunneling and its dependence on the bias voltage and the position of the tip with respect to the sample. The electrons transfer from the tip to the sample or vice versa depending upon the sign of the bias voltage V. At large tip-sample distances it is reasonable to neglect the tip-sample interaction or account for it by some perturbative method such as Bardeen's.[8] However, as the tip is moved closer to the sample resulting in more tip-sample interactions, the electron clouds of both the tip and the sample adjust extensively to the presence of each other. To account for this relaxation, we treat the entire STM-STS system (i.e., tip, sample, etc.) as a many-body problem (all electrons and nuclei) and think of the system as a supermolecule. Tip and sample are dealt with on equal foot-

ing. Of course, in the limit of large tip-sample distances, results using the supermolecule model should be identical to those from the other models. The theoretical work of Ciraci *et al.*[14] is the only other one with the same general intent as ours. These authors, however, concerned themselves mostly with the energetics of the system—not with its electron-transfer properties.

A. The electronic coupling matrix element

In the supermolecule approach the STM-STS tunneling is an electron transfer (ET) *within* the supermolecule. Moreover, at large tip-sample separation, the tunneling is mostly "through space" instead of "through bond," since there are no chemical bonds between the tip and the sample to mediate the transfer of the electrons. In other words, the tunneling here is primarily due to the spatial overlap of the wave function of the system in the initial state of ET with that of the final state of ET.[15] For different theories and applications of electron transfer, the reader is referred to the large body of literature in the field.[16]

A key quantity in theory of ET is the so-called electron-transfer (or electronic coupling) matrix element given as[17–19]

$$T_{ab}=\frac{\left|H_{ab}-S_{ab}\left[\frac{H_{aa}+H_{bb}}{2}\right]\right|}{1-S_{ab}^2}\ , \tag{1}$$

where $H_{ab}=\langle\psi_a|H|\psi_b\rangle$, $S_{ab}=\langle\psi_a|\psi_b\rangle$, $H_{aa}=\langle\psi_a|H|\psi_a\rangle$, $H_{bb}=\langle\psi_b|H|\psi_b\rangle$, and H is the total Born-Oppenheimer (i.e., excluding nuclear kinetic energy) Hamiltonian of the system, ψ_a represents the full many-electron wave function of the entire system before (or after) electron transfer, and ψ_b is that for after (or before) electron transfer. As the name implies, T_{ab} given by Eq. (1) is a measure of the strength of the coupling between the charge-transfer states $|\psi_a\rangle$ and $|\psi_b\rangle$. In fact, T_{ab} appears, one way or another, in classical,[20] semiclassical,[21] and quantum-mechanical[22,17] treatment of ET. Note that the tunneling current I and T_{ab} are related, at large tip-sample distances, through the well-known expression[4–8]

$$I=\frac{2\pi e}{\hbar}\sum_{a,b}f(E_a)[1-f(E_b+eV)]|T_{ab}|^2\delta(E_a-E_b)\ , \tag{2}$$

which results from using first-order time-dependent perturbation theory. Here, $f(E)$ is the Fermi distribution function of the sample surface, E_a and E_b are eigenvalues of ψ_a and ψ_b, respectively, and the constants have their usual meanings. In the limits of low temperature (room temperature or below) and low bias voltage V which are consistent with the experimental conditions,

$$I=\frac{2\pi e^2V}{\hbar}\sum_{a,b}|T_{ab}|^2\delta(E_b-E_F)\delta(E_a-E_F)\ , \tag{3}$$

where E_F is the Fermi level. We see that the tunneling current I is proportional to the applied voltage V and explicitly dependent on the square of the electronic coupling matrix element T_{ab}. Observe that Eq. (1) reflects the essential symmetry with respect to the arbitrary labels a and b. This is the so-called *reciprocity principle* in STM literature which states that STM images are invariant upon interchange of the tip state with the sample state.[6]

The main purpose of this initial study is to see to what extent the topography of the sample charge density manifests itself in that of T_{ab} or $|T_{ab}|^2$. The latter appears in Eq. (2). More specifically, we would like to assess the changes in T_{ab} caused by changes in the chemical nature and size of the sample. In addition, we study the effect of the applied voltage on T_{ab} and see how the latter varies with the tip-sample distance.

B. The computational model

First, we model the sample with a single molecule in vacuum. This represents no liability for the main objective of this study which attempts to relate any arbitrary sample charge distribution to its T_{ab}. The model, however, may also be appropriate for imaging of an adsorbed molecule. Our assumption is that the critical process in STM-STS imaging is the initial electron exchange between the adsorbed molecule and the tip, which is thus responsible for the qualitative features of the image of the adsorbed molecule. Additionally, we assume that the effect of the adsorbing surface is small. Indeed, the molecule is not drowned in the sea of the surface, as demonstrated by the fact that experimentally adsorbed molecules usually can be discerned.[23] However, for chemisorbed molecules that are chemically bound to the surface, such as for an oxidized state of silicon surface,[24] the surface cannot be neglected as it is an integral part of the system. A cluster representation of the system would replace the molecule used here. In this preliminary investigation we choose formic acid HCOOH as the molecule, because of its varied chemical structure. It has both double and single bonds and has identical atoms in different chemical environments. As shown in Fig. 1, the model molecule has a charge distribution which shows varied

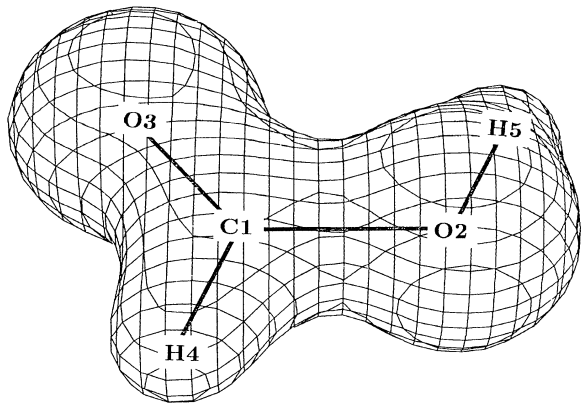

FIG. 1. Surface of the total electronic charge density of formic acid HCOOH at 0.1 a.u.

topographical features. Incidentally, we note that a molecule of sorbic acid, i.e., with the same functional group, adsorbed on a surface was seen by atomic force microscopy (AFM).[25]

Second, in keeping with the accepted belief that only the "last" atom on the tip is STM active, the tip is modeled by a single atom. The choice of the type of metal atom (in our case, a zinc atom) was made on the basis of ease of computation. Note that the two states involved in the electron transfer, namely, ψ_a and ψ_b, ψ_a is the quasidiabatic solution of the Schrödinger equation charge localized on the molecule (or the metal atom) and ψ_b is the quasidiabatic solution charge localized on the metal atom (or the molecule). To model the transfer of electron between the tip and the molecule, the whole system is positively charged. Thus, one state of the supermolecule is of the form $\{HCOOH\}$-Zn^+ and the other of the form $\{HCOOH\}^+$-Zn. The electronic configuration of Zn is $[Ar]3d^{10}4s^2$ and of Zn^+ is $[Ar]3d^{10}4s^1$ with closed p and d shells. Other more "realistic" tip atoms such as W, Ni, and Pt with their open d shells will be investigated at a later stage. Additionally, this would provide a means to explore the relationship between STM image and charge density for "spherically symmetric" as well as "nonspherically symmetric" tip atoms. A small cluster representation of the tip could also be used; however, as seen below, it appears that there is a lot to be learned from the present model.

C. Computational details

All the results reported here are based on open-shell spin unrestricted Hartree-Fock (UHF) quasidiabatic charge-localized wave functions using the HONDO molecular program.[26] We use Eq. (1) to compute the values of the electronic coupling matrix element T_{ab}. The latest version of HONDO actually outputs off-diagonal elements H_{ab}, S_{ab} in addition to the usual total energies H_{aa} and H_{bb}. The computational method for the off-diagonal elements used in HONDO is described in detail by Farazdel *et al.*[19] Initially, an equilibrium shape for formic acid was determined by the geometry optimization procedure. This planar geometry was then kept fixed for all our calculations while varying the position of the tip with respect to the plane of the formic acid molecule. This is consistent with the Condon approximation[27] according to which T_{ab} is assumed to be only weakly dependent on configuration of the molecule as long as the donor-acceptor distance in the charge-transfer molecule remains unchanged.[19]

For each and every position of the "tip," we calculated the two quasidiabatic SCF wave functions $|\psi_a\rangle$ and $|\psi_b\rangle$ with charge localized on either side (i.e., formic acid or zinc atom). To this end, we closely monitored charge and spin populations at every tip-sample distance. The two wave functions are nonorthogonal, the one with the positive charge localized on the sample corresponding to the charge-transfer state (or excited state). Convergence of these SCF wave functions requires using the powerful DIIS algorithm[28] in addition to using the converged molecular orbitals obtained for a nearby geometry. The basis sets used throughout our calculations are 4-21G (Ref. 29) for atoms H, C, O, and Huzinzga's 43321/43/31 (Ref. 30) for Zn. These are double-zeta quality basis sets and should suffice for qualitative results. More accurate values of T_{ab}, mainly at large distances, would require more diffuse functions.[18]

III. RESULTS AND DISCUSSION

A. Variation of T_{ab} with d

Calculated T_{ab} values as a function of the tip-sample distance d are displayed in Fig. 2(a) for five lateral positions on the sample. These positions are directly above the carbon atom C1, the hydroxyl oxygen atom O2, the carbonyl oxygen atoms O3, the formyl hydrogen atom H4, and the hydroxyl hydrogen atom H5. Figures 2(b) and 2(c) show the same curves as in Fig. 2(a), but obtained when a uniform electric field perpendicular to the sample is applied in the calculation in the direction of the sample toward the tip. The filed intensities are 0.001 and 0.002 a.u. (or $\simeq$0.05 and 0.1 V/Å, respectively). Note that, as d decreases, some of the curves terminate earlier than others. This is due to the inability to converge the SCF process for positions beyond the last point on the curve. In the calculation the charge-transfer (excited) state would collapse to the ground state as the computational procedure contains nothing that prevents such a collapse.

All the curves display the same characteristic of a broad peak between 9.0 and 2.5 Å, then a sharp peak at short distances. The height of the peak depends on the lateral position of the approach. In both cases with and without the external field, the height of the peak for the vertical approach above the carbonyl oxygen is at most half of the height for approaching above the other atoms. This is actually quite surprising considering the molecular orbitals involved in the electron transfer, as discussed below. The key orbital is indeed localized on the carbonyl oxygen O3, but is orientation is in the plane of the molecule, more so than along the direction of approach. Finally, we note that the onset of the broad peak, for the calculations involving the external electric field, is at about 7 Å, instead of 9 Å. The general features of the curves are otherwise the same, with broad and sharp peaks. The following three points should be made:

(1) The feature of broad and sharp peaks reveals that two processes of different chemical nature take place. Their character can be established by analyzing the molecular orbitals that make up the initial and the final state. The analysis is done below. The operating range of STM-STS seems to correspond to the domain of the broad peak, i.e., >3 Å.

(2) The broad peaks observed between 3 and 9 Å are different depending on the vertical approaches. Already, we see hints of being able to calculate surfaces of constant T_{ab}, which will correlate with the chemical structure of the sample. To this end, we need to sample a large number of geometries of the supermolecule.

(3) The general features are maintained in going from no electric field to a small electrical field. Thus, the "image" is not field sensitive in a qualitative sense.

B. Variation of S_{ab} and H_{ab} with d

Since at large tip-sample distances we expect the charge transfer to have a strong dependence on the overlap between the initial- and the final-state wave function, we give in Figs. 3 and 4 the variations of S_{ab} and H_{ab} with d. Most remarkably, the general features observed for T_{ab} appear also for both S_{ab} and H_{ab}. This suggests that one should get a qualitative understanding of the STM image from analysis of the overlap S_{ab}. Of course, S_{ab} depends strongly on the chemical structure of the sample; the analysis for the case of formic acid is given below. In light of the resemblance between T_{ab}, S_{ab}, and H_{ab}, it is useful to consider the ratio $H_{ab}/S_{ab}(H_{aa}+H_{bb})$, keeping in mind Mulliken's approximation,[31] which states that

$$H_{ab} \simeq CS_{ab}(H_{aa}+H_{bb}) , \tag{4}$$

where C is a constant. Now Eq. (1) can be rewritten as

$$T_{ab} \simeq \frac{S_{ab}}{1-S_{ab}^2}(H_{aa}+H_{bb})(C-\tfrac{1}{2}) . \tag{5}$$

For all tip-sample distances considered in this study, and for all lateral positions of the tip, we found C to be very close to 0.5 within a few parts per thousand, with the deviation from 0.5 contributing minimally to the shape of

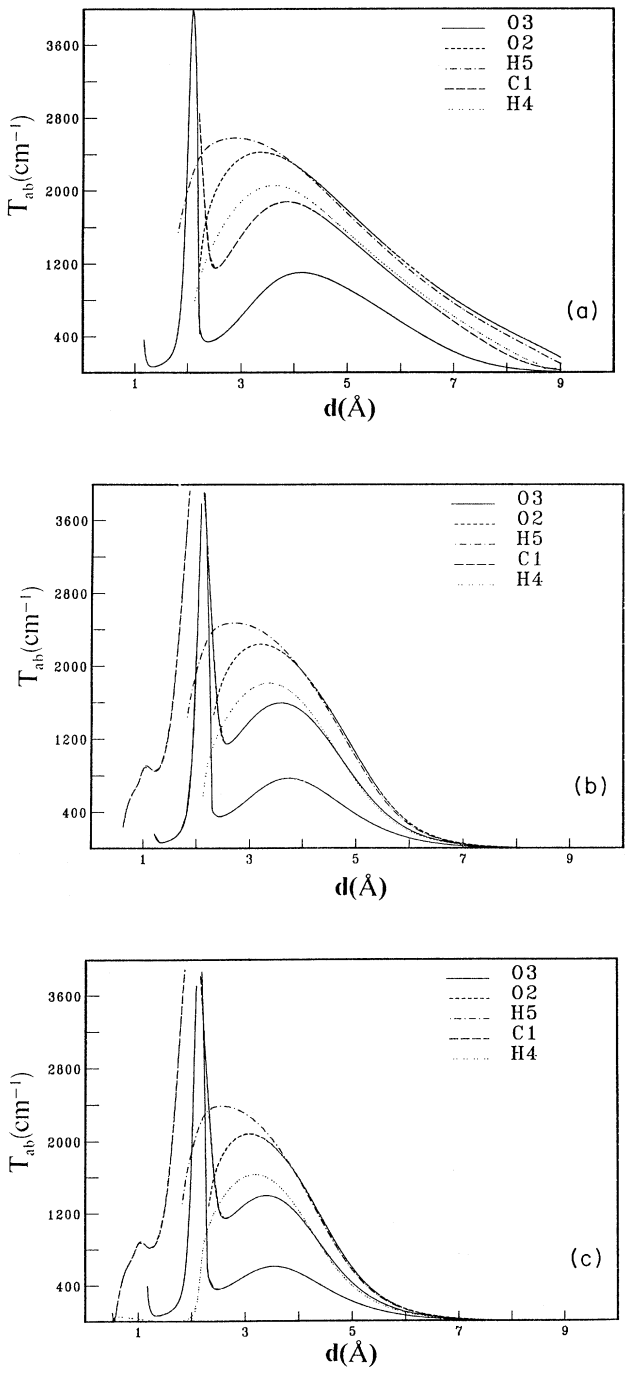

FIG. 2. Variation of the electronic coupling matrix element T_{ab} vs tip-sample distance d. Electric-field strength: (a) 0.000 a.u., (b) 0.001 a.u., and (c) 0.002 a.u.

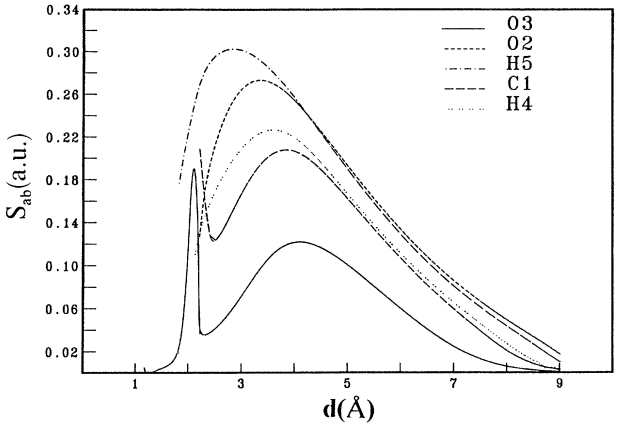

FIG. 3. Variation of the overlap S_{ab} vs tip-sample distance d at zero field.

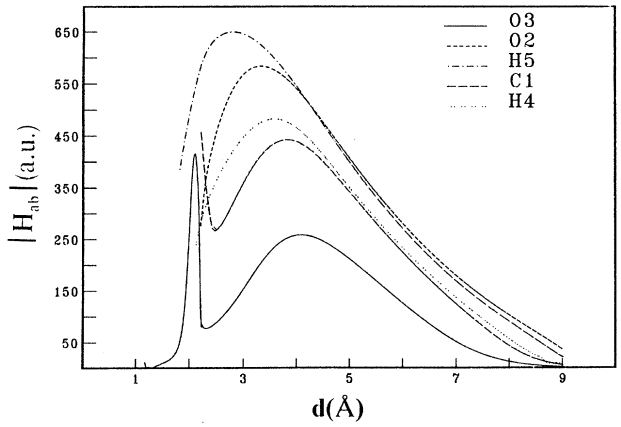

FIG. 4. Variation of H_{ab} vs tip-sample distance d at zero field.

T_{ab}. This finding is consistent with the fact that the shape of T_{ab} is primarily due to the shape of S_{ab} [compare Fig. 2(a) with Fig. 3]. Finally, we should mention that S_{ab} and H_{ab} have almost identical shapes (compare Fig. 3 with Fig. 4). This is because the $C(H_{aa}+H_{bb})$ values in Eq. (4) are practically a constant at large d and monotonically increases as d decreases at small values.

C. Molecular-orbital-theory considerations

The following considerations result from analysis of the SCF wave function of the ground state of the system {HCOOH}-Zn^+. The three highest occupied molecular orbitals (HOMO's) have the following characters. In increasing order of energy we find a π orbital delocalized over the p_z functions of the two oxygen atoms with a nodal plane passing through the carbon atom (z is the direction perpendicular to the molecular plane). Next comes an orbital localized on the carbonyl oxygen and lying in the plane of the molecule. This is a lone-pair orbital l_p containing a carbonyl-oxygen lone pair of electrons, as shown in Fig. 5. Then we find the 4s orbital of the zinc atom with only one electron (spin α). The lowest unoccupied molecular orbital (LUMO) is an antibonding π^* orbital delocalized over the O=C—O frame. The ordering of the orbitals is in accord with the spectroscopic data[32] about formic acid which place the $n\rightarrow\pi^*$ excitation at about 5 eV above the ground state and the $\pi\rightarrow\pi^*$ excitation at 8 eV. The ionization potential of formic acid is 11.3 eV and for zinc it is 9.4 eV. Thus the ground-state wave function can be abbreviated as

$$\psi(M-Zn^+)=A\,(\text{core}\,\pi\,\bar{\pi}\,lp\,\bar{lp}4s) \tag{6}$$

and for the excited charge-transfer state,

$$\psi(M^+-Zn)=A\,(\text{core}\,\pi\,\bar{\pi}\,lp\,4s\,\bar{4s})\,, \tag{7}$$

where A is the usual antisymmetrizer and "core" represents all other inner and valence orbital electrons. The latter state is denoted by $\psi(lp\rightarrow 4s)$. The next excited state of the supermolecule at large distance corresponds to a $\pi\rightarrow 4s$ excitation, which is also a charge-transfer state. The fourth excited state of the supermolecule corresponds to a $\pi\rightarrow\pi^*$ excitation. This is not a charge-transfer state; it is simply a complex made of HCOOH ($\pi\rightarrow\pi^*$) state with Zn^+.

A small configuration-interaction (CI) calculation of the energies of these four states as a function of the tip-sample distance d yields the curves shown in Fig. 6. These curves are semiquantitative but reveal the following information: At large distances we recognize the ground state, the $lp\rightarrow 4s$ state, the $n\rightarrow 4s$ state, and the $\pi\rightarrow\pi^*$ state, in this order of increasing energy. As the distance d decreases, we observe that all the curves are only slowly changing until 3.7 Å. The ground state changes slowly until 2.7 Å where it becomes repulsive. The excited-state energies change more significantly starting at 3.7 Å and clearly display an avoided curve crossing involving all three excited states. The avoided crossing occurs at 2.2 Å, and from then on, the first excited state can be labeled as $\pi\rightarrow\pi^*$, a non-charge-transfer state. This characterization is corroborated by studying the SCF orbitals of the excited state for which we calculate S_{ab}. At long range Eqs. (6) and (7) show that S_{ab} is nearly equal to the overlap between the two orbitals involved in the charge transfer, i.e., l_p and 4s orbitals. Thus,

$$S_{ab}\simeq(lp\,|\,4s)\,. \tag{8}$$

At about 2.3 Å the orbitals involved in the electronic transition change character dramatically, as reflected in the avoided curve crossing. The quantity S_{ab} is now best approximated by

$$S_{ab}\simeq(\pi\,|\,\pi^*)\,, \tag{9}$$

and the calculations show that the upper state in the transition has a charge localization on the Zn atom just as for the ground state, and that the sample fragment

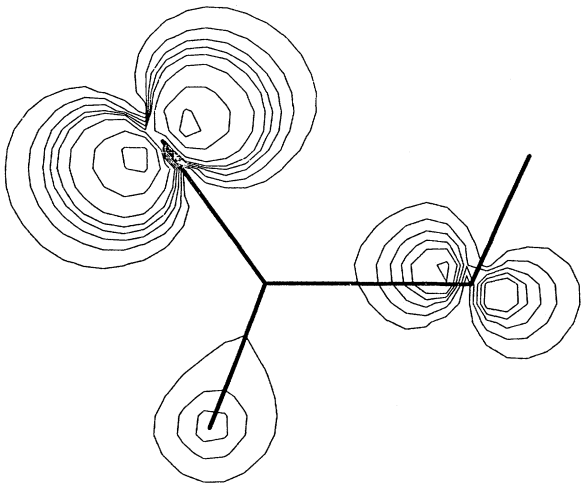

FIG. 5. A contour charge-density map of the lone-pair orbital localized on the carbonyl oxygen O3 (see Fig. 1 for atomic label scheme).

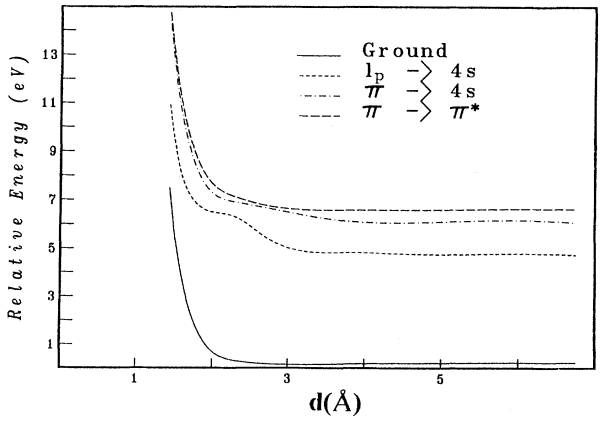

FIG. 6. Energy curves of four electronic states of the {HCOOH-Zn}$^+$ system as a function of the tip-sample distance d.

resembles the $\pi \rightarrow \pi^*$ excited state of formic acid. The sharp peak for T_{ab} at short distance thus *does not* correspond to a charge-transfer state from the sample to the tip, but rather to an "intrasample" transfer, i.e., an excitation. In the STM perspective, then, one should focus only on the outer peak which corresponds to the transfer of a lone-pair electron to the metal atom of the tip. Whether the inner peak may have any significance in STM experiments is an open question. Note additionally that all throughout this work the geometry of the sample molecule was kept fixed to its parameters of an isolated molecule, a reasonable assumption for large tip-sample distances. At shorter distances geometry relaxation of the sample may have to be taken into account.

Our present findings confirm the key role of overlap quantities in providing a qualitative understanding of the physics of STM. In particular, the HOMO and LUMO orbitals localized on the sample and their electron distributions may give an "image" of the sample similar to the one created in STM experiments. Such is the case for the recent work of Smith *et al.*[33] In their case the HOMO was a π orbital. As shown in our study, where the HOMO is an in-plane lone-pair orbital, there is no requirement that the useful orbital will always be π type. Instead, the key orbital is found to be intimately connected to the chemical structure of the sample.

IV. CONCLUSION

We have presented a supermolecule approach to the modeling of STM-STS. Our focus has been on the electron-transfer process and we used *ab initio* all-electron SCF wave functions to describe the initial and final states of the system. Our results indicate that the electron-transfer process reflects the chemical environment of the precursor sample. We showed that the electronic structure of the sample molecule is intimately linked to the electron tunneling process. A qualitative analysis of the states involved in the transition yields an expression for the overlap quantity which reflects the key features of the electron-transfer process.

Future work involves generating surfaces of constant electron-transfer coupling T_{ab} and analyzing those to understand the topography of the sample. In addition, work is needed to further our understanding of the mechanism of electron transfer for short tip-sample distances.

---

*Present address: 301 Trinity Court No. 1-7, Princeton, NJ 08540-7021.

[1]G. Binnig, H. Rohrer, C. Gerber, and E. Weibel, Phys. Rev. Lett. **49**, 57 (1982); G. Binnig and H. Rohrer, Helv. Phys. Acta **55**, 726 (1982); Surf. Sci. **126**, 236 (1983); **152-153**, 17 (1985); IBM J. Res. Dev. **30**, 355 (1986).

[2]*Scanning Tunneling Microscopy and Related Techniques,* edited by R. J. Behm, N. Garcia, and H. Rohrer (Kluwer Academic, Boston, 1990).

[3]A. Baratoff, Physica B **127**, 143 (1984).

[4]J. Tersoff and D. R. Hamann, Phys. Rev. Lett. **50**, 1998 (1983).

[5]J. Tersoff and D. R. Hamann, Phys. Rev. B **31**, 805 (1985).

[6]C. J. Chen, J. Vac. Sci. Technol. A **6**, 319 (1988).

[7]C. J. Chen, Phys. Rev. Lett. **65**, 448 (1990); Mat. Res. Soc. Symp. Proc. **159**, 289 (1990); Phys. Rev. B **42**, 8841 (1990).

[8]J. Bardeen, Phys. Rev. Lett. **6**, 57 (1961).

[9]J. Callaway and N. H. March, in *Solid State Physics,* edited by H. Ehrenreich, F. Seitz, and D. Turnbull (Academic, New York, 1984), Vol. 38, pp. 135.

[10]M. Tsukada and N. Shima, J. Phys. Soc. Jpn. **56**, 2875 (1987); M. Tsukada, N. Shima, S. Ohnishi, and Y. Chiba, J. Phys. (Paris) Colloq. **6**, C11-91 (1987); S. Ohnishi and M. Tsukada, Solid State Commun. **71**, 391 (1989); J. Vac. Sci. Technol. A **8**, 174 (1990); M. Tsukada and K. Kobayashi, J. Vac. Sci. Technol. A **8**, 160 (1990); K. Kobayashi and M. Tsukada, *ibid.* **8**, 170 (1990).

[11]A. A. Lucas, H. Morawitz, G. R. Henry, J. P. Vigneron, P. Lambin, P. H. Cutler, and T. E. Feuchtwang, Solid State Commun. **65**, 1291 (1988); Phys. Rev. B **37**, 10 708 (1988).

[12]C. Noguera, Phys. Rev. B **42**, 1629 (1990).

[13]G. Doyen, D. Drakova, E. Kopatzki, and R. J. Behm, J. Vac. Sci. Technol. A **6**, 327 (1988); G. Doyen, E. Koetter, J. P. Vigneron, and M. Scheffler, Appl. Phys. A **51**, 281 (1990).

[14]S. Ciraci and I. P. Batra, Phys. Rev. B **36**, 6194 (1987); I. P. Batra and S. Ciraci, J. Vac. Sci. Technol A **6**, 313 (1988); E. Tekman and S. Ciraci, Phys. Scr. **38**, 486 (1988); Phys. Rev. B **40**, 10 286 (1989); S. Ciraci, A. Baratoff, and I. P. Batra, *ibid.* **41**, 2763 (1990); **42**, 7618 (1990).

[15]We are implying the two-state model here, i.e., it is assumed that only two electronic states, the state before and the state after ET, need be considered and the coupling with other states is neglected.

[16]See, for example, the following review articles: R. R. Dogonadze, A. M. Kuznetsov, and T. A. Maragishvili, Electrochim. Acta **25**, 1 (1980); N. Sutin, Prog. Inorg. Chem. **30**, 441 (1983); M. D. Newton and N. Sutin, Annu. Rev. Phys. Chem. **35**, 437 (1984); K. V. Mikkelsen and M. A. Ratner, Chem. Rev. **87**, 113 (1987).

[17]N. R. Kestner, J. Logan and J. Jortner, J. Phys. Chem. **78**, 2148 (1974).

[18]R. J. Cave, Ph.D. thesis, California Institute of Technology, 1986, Chap. 1; R. J. Cave, D. V. Baxter, W. A. Goddard III, and J. D. Baldeschwieler, J. Chem. Phys. **2**, 926 (1987).

[19]A. Farazdel, M. Dupuis, E. Clementi, and A. Aviram, J. Am. Chem. Soc. **112**, 4206 (1990).

[20]R. A. Marcus, J. Chem. Phys. **24**, 966 (1956); Can. J. Chem. **37**, 155 (1959); Discuss. Faraday Soc. **29**, 21 (1960); N. S. Hush, Trans. Faraday Soc. **57**, 155 (1961); R. A. Marcus, J. Annu. Rev. Phys. Chem. **15**, 155 (1964); J. Chem. Phys. **43**, 679 (1965); Electrochim. Acta **13**, 995 (1968); E. Waisman, G. Worry, and R. A. Marcus, J. Electroanal. Chem. **82**, 9 (1977).

[21]B. S. Brunschwig, J. Logan, M. D. Newton, and N. Sutin, J. Am. Chem. Soc. **102**, 5798 (1980).

[22]S. P. Dolin, E. D. German, and R. R. Dogonadze, J. Chem. Soc. Faraday Trans. 2 **73**, 648 (1977); M. D. Newton, Int. J. Quantum Chem. Quantum Chem. Symp. **14**, 363 (1980).

[23]P. Avouris, J. Phys. Chem. **94**, 2246 (1990).

[24]I. W. Lyo, P. Avouris, B. Schubert, and R. Hoffman, J. Phys. Chem. (to be published).

[25]B. Drake, C. B. Prater, A. L. Weisenhorn, S. A. C. Gould, T.

R. Albrecht, C. F. Quate, D. S. Cannell, H. G. Hansma, and P. K. Hansma, Science **243**, 1586 (1989).

[26]M. Dupuis, J. Rys, and H. F. King, J. Chem. Phys. **65**, 111 (1976); M. Dupuis, A. Farazdel, S. P. Karna, and S. A. Maluendes, in *Modern Techniques in Computational Chemistry,* edited by E. Clementi (ESCOM Science, Leiden, 1990), pp. 277.

[27]J. Ulstrup, *Charge Transfer Processes in Condensed Media* (Springer-Verlag, New York, 1979).

[28]T. P. Hamilton and P. Pulay, J. Chem. Phys. **84**, 5728 (1986).

[29]J. S. Binckley, J. A. Pople, and W. J. Hehre, J. Am. Chem. Soc. **102**, 939 (1980); M. S. Gordon, J. S. Binckley, J. A. Pople, and W. J. Pietro, *ibid.* **104**, 2797 (1982).

[30]*Gaussian Basis Sets for Molecular Calculations,* edited by S. Huzinaga (Elsevier Science, New York, 1984).

[31]W. Person and R. Mulliken, *Molecular Complex,* (Wiley, New York, 1969); A. Aviram, J. Am. Chem. Soc. **110**, 5687 (1988).

[32]G. Herzberg, *Molecular Spectra and Molecular Structure of Polyatomic Molecules,* (Van Nostrand, New York, 1966).

[33]D. P. E. Smith, J. K. H. Hörber, G. Binnig, and H. Nejoh, Nature **344**, 641 (1990).